physical sciences forum

Proceeding Paper

Searches for Dark Matter in the Galactic Halo and Extragalactic Sources with IceCube

Minjin Jeong

MDPI

https://doi.org/10.3390/psf2023008070

physical sciences forum

MDPI

Proceeding Paper

Searches for Dark Matter in the Galactic Halo and Extragalactic Sources with IceCube †

Minjin Jeong on behalf of the IceCube Collaboration

Department of Physics, Sungkyunkwan University, Suwon 16419, Republic of Korea; minjin.jeong@g.skku.edu

† Presented at the 23rd International Workshop on Neutrinos from Accelerators (NuFACT 2022), Salt Lake City, UT, USA, 30–31 July 2022.

Abstract: Although there is overwhelming evidence for the existence of dark matter, the nature of dark matter remains largely unknown. Neutrino telescopes are powerful tools to search indirectly for dark matter, through the detection of neutrinos produced during dark matter decay or annihilation processes. The IceCube Neutrino Observatory is a cubic-kilometer-scale neutrino telescope located under 1.5 km of ice near the Amundsen-Scott South Pole Station. Various dark matter searches were performed with IceCube over the last decade, providing strong constraints on dark matter models. In this contribution, we present the latest results from IceCube as well as ongoing analyses using IceCube data, focusing on the works that look at the Galactic Halo, nearby galaxies, and galaxy clusters.

Keywords: dark matter; neutrinos; IceCube

1. Introduction

The IceCube Neutrino Observatory [1] is a cubic-kilometer-scale neutrino telescope, deployed in deep glacial ice in Antarctica. The telescope consists of 86 vertically placed strings that are 125 m apart from each other. Each of the strings holds 60 digital optical modules (DOMs) that contain a downward-facing photomultiplier tube (PMT) and readout electronics. The DOMs are deployed at depths between 1450 m and 2450 m, utilizing the ultra-transparent Antarctic ice as Cherenkov medium. In most of IceCube, the DOMs on the same string are spaced 17 m apart, but at the bottom center of the detector, they are more densely spaced with a spacing of 7 m. This densely spaced sub-array is called the DeepCore and was designed to detect low-energy neutrino events. At the surface of IceCube, the IceTop air-shower detector array is located. This surface array was designed to observe cosmic rays and is also used to veto atmospheric backgrounds for IceCube.

IceCube can probe dark matter models by looking for neutrinos produced by dark matter interactions. When dark matter in an astronomical object self-annihilates or decays into Standard Model particles, neutrinos could be produced directly or indirectly, and a flux of these neutrinos could be observed at IceCube. Multiple analyses were performed using IceCube data to search for dark matter in the Sun [2,3], the Earth [4,5], the Milky Way [6–11], and extragalactic sources [12], deriving competitive constraints on the dark matter models. We present dark matter searches with IceCube, which were completed recently or are in progress. The presented analyses focus on dark matter interactions in the our Galaxy or extragalactic sources.

2. HESE 7.5-Year Analyses

We performed analyses using IceCube's 7.5-year High-Energy Starting Event (HESE) sample [13] to search for dark matter interactions. The HESE event selections achieve a high purity of astrophysical neutrinos, and the data sample contains track-like events and cascade events from all directions. Details of the event selections can be found from

Citation: Jeong, M., on behalf of the IceCube Collaboration. Searches for Dark Matter in the Galactic Halo and Extragalactic Sources with IceCube. *Phys. Sci. Forum* **2023**, *8*, 70. https://doi.org/10.3390/psf2023008070

Academic Editor: Yue Zhao

Published: 5 December 2023

Reference [13]. In the first analysis, we searched for neutrinos from dark matter decay or self-annihilation. In the second analysis, we looked for evidence of the scattering of high-energy astrophysical neutrinos with dark matter in our galaxy. In both of the works, we model the dark matter distribution in our galaxy by taking the parameterization presented in Reference [14], which is based on the Einasto profile [15].

For the decaying dark matter search, we consider dark matter with masses from 160 TeV and 20 PeV. Also, dark matter is assumed to decay into $b\bar{b}$, W^+W^-, $\tau^+\tau^-$, $\mu^+\mu^-$, $H\nu$, or $\nu\bar{\nu}$ with 100% branching ratio. We account for signals from cosmological dark matter decay as well as Galactic dark matter decay. In this case, the signal neutrino flux is evaluated as the following:

$$\frac{d\Phi_\nu}{dE_\nu} = \frac{d\Phi_\nu^{\mathrm{Gal}}}{dE_\nu} + \frac{d\Phi_\nu^{\mathrm{Cos}}}{dE_\nu}. \tag{1}$$

The Galactic contribution $\frac{d\Phi_\nu^{\mathrm{Gal}}}{dE_\nu}$ is calculated as

$$\frac{d\Phi_\nu^{\mathrm{Gal}}}{dE_\nu} = \frac{1}{4\pi m_\chi \tau_\chi} \frac{dN_\nu}{dE_\nu} \int_{l.o.s} \rho_\chi(s) ds, \tag{2}$$

where m_χ is the dark matter mass, τ_χ is the dark matter lifetime, $\frac{dN_\nu}{dE_\nu}$ is the neutrino production spectrum. The dark matter density (ρ_χ) is integrated along the line-of-sight. The cosmological contribution $\frac{d\Phi_\nu^{Cos}}{dE_\nu}$ is as follows:

$$\frac{d\Phi_\nu^{Cos}}{dE_\nu} = \frac{\Omega_\chi \rho_c}{4\pi m_\chi \tau_\chi H_0} \int_0^\infty \frac{dN_\nu}{dE_\nu(1+z)} \frac{dz}{\sqrt{\Omega_\lambda + \Omega_m(1+z)^3}}, \tag{3}$$

where ρ_c is the critical density of the Universe, H_0 is the Hubble constant, z is the redshift, and Ω_Λ, Ω_χ, and Ω_m are the energy density, cold dark matter density, and matter density, respectively. We disregard the contribution from extragalactic dark matter clumps, making the analysis results conservative. A binned maximum likelihood analysis is performed, which uses energy and directional information as observables. Backgrounds are estimated from Monte Carlo simulation. More details of the analysis methods are presented in Reference [16].

For the annihilating dark matter search, we probe dark matter masses ranging from 80 TeV to 10 PeV. Various dark matter decay channels, including $b\bar{b}$, W^+W^-, $\mu^+\mu^-$, and $\nu\bar{\nu}$, are studied. We only consider the Galactic dark matter annihilation, as it is expected to dominate the signal flux. Then, the signal neutrino flux is calculated as

$$\frac{d\Phi_\nu}{dE_\nu} = \frac{\langle \sigma v \rangle}{8\pi m_\chi} \frac{dN_\nu}{dE_\nu} \int_{l.o.s} \rho_\chi^2(s) ds, \tag{4}$$

where $\langle \sigma v \rangle$ denotes the velocity-averaged dark matter annihilation cross-section.

In this work, the neutrino spectrum, $\frac{dN_\nu}{dE_\nu}$, is simulated using PYTHIA [17], partially taking into account electroweak corrections. To account for halo model uncertainties, the NFW and Burkert models presented in Reference [18] are also studied.

Figure 1 shows upper limits on the velocity-averaged dark matter annihilation cross-section obtained from this analysis. The limits calculated at 90% C.L. for different decay channels are shown in the left panel. In the right panel, the limits for the $\mu^+\mu^-$ channel are compared to those from previous experiments. In Figure 2, lower limits on the dark matter lifetime are shown in the same manner as Figure 1. It can be seen that the limits from this analysis are highly stringent for the probed dark matter masses.

To search for evidence of dark matter–neutrino scattering, we use the energy and directional distribution of the HESE events. We assume that the extragalactic neutrino flux has an unbroken power-law spectrum. The energy and directional distribution of the neutrino flux are expected to change when the neutrinos scatter on the Galactic dark matter, depending on the dark matter mass, mediator mass, Galactic dark matter distribution, and the couplings of dark matter and neutrino to the mediator. We consider two simplified

dark matter–neutrino scattering scenarios: fermionic dark matter with a vector mediator and scalar dark matter with a fermionic mediator. We assume that the scattering between dark matter particles and neutrinos is elastic and neglect secondary neutrinos from the interaction (see Reference [16] for more details of the signal expectation and analysis method). Since no evidence for the dark matter interaction was found, we derived constraints on the dark matter–neutrino scattering for the two scattering scenarios, which can be found in Figure 3.

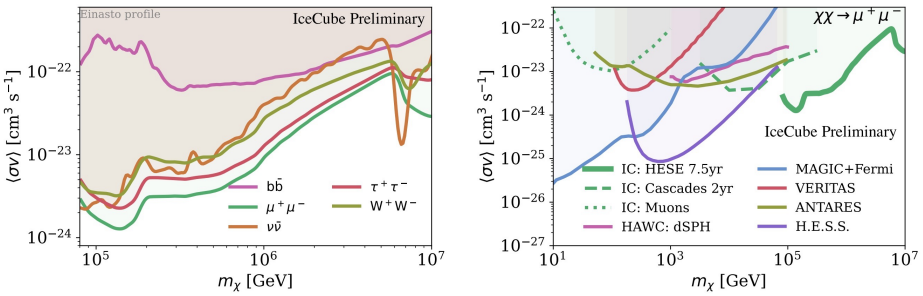

Figure 1. Upper limits (90% C.L.) on the velocity-averaged dark matter self-annihilation cross-section. Left panel shows the limits obtained from the HESE 7.5-year analysis for the considered dark matter annihilation channels and the Einasto halo model. In the right panel, the limits for the $\mu^+\mu^-$ channel are compared with limits from other experiments [19–24]. These plots are taken from [16].

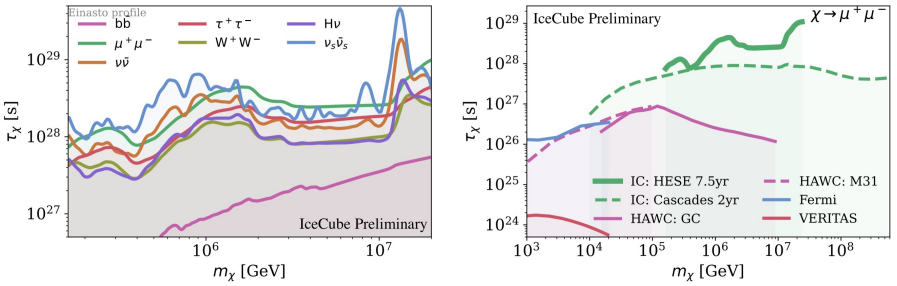

Figure 2. Lower limits (90% C.L.) on the dark matter lifetime. Left panel shows the limits obtained from the HESE 7.5-year analysis for the considered dark matter decay channels and the Einasto halo model. In the right panel, the limits obtained for the $\mu^+\mu^-$ channel are compared with limits from other experiments [19–24]. These plots are taken from Reference [16].

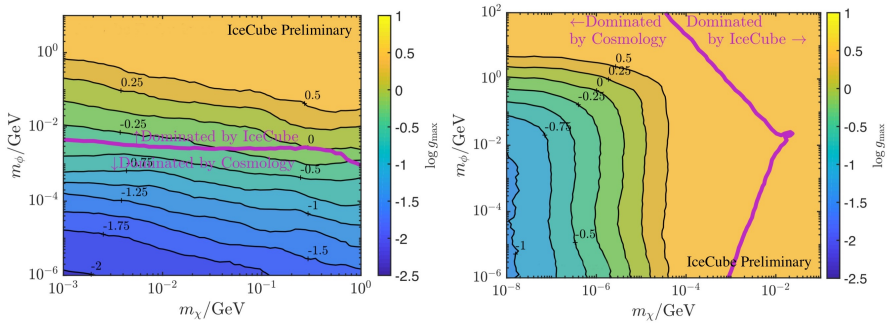

Figure 3. Credible upper limits (90%) on the maximum dark matter–neutrino coupling strength, obtained from the HESE 7.5-year analysis. Left panel shows the limits for fermionic dark matter with a vector mediator scenario. Right panel shows the limits for the scalar dark matter with a fermionic mediator scenario. In each of the panels, the limits are shown as a function of the mediator mass (m_ϕ) and dark matter mass (m_χ). The pink line separates the regions of parameter space where cosmology or IceCube gives stronger bounds. The plots are taken from Reference [16].

3. Neutrino Line Analysis

This analysis searches for low-to-medium energy neutrinos from dark matter annihilation or decay in the Galactic Center. The expected signal neutrino flux is calculated using Equation (2). Two different halo models are considered: the NFW model and the Burkert model presented in Reference [18]. The considered dark matter masses range from 10 GeV to 40 TeV, and the analysis is optimized to detect signals from the $\chi \to \nu\bar{\nu}$ or $\chi\chi \to \nu\bar{\nu}$ scenario where the signal neutrino spectrum consists of a delta-function at $E_\nu = m_\chi$ (annihilation) or $E_\nu = m_\chi/2$ (decay). In addition to the $\nu\bar{\nu}$ channel, the $b\bar{b}$, W^+W^-, $\mu^+\mu^-$, and $\tau^+\tau^-$ channels are also probed. We use the signal neutrino spectra calculated in PPPC4 [25], which accounts for leading-order electroweak corrections.

For this work, 5 years of data collected from 2012 to 2016 is used. To achieve a good energy resolution, the event selection is optimized to select cascade events starting in the DeepCore sub-array. The neighboring IceCube DOMs are used as a veto. Two sub-samples are produced by the final event selection. The low-energy sample is obtained using a BDT trained with the signal spectrum expected from the $m_\chi = 100$ GeV, $\chi \to b\bar{b}$ scenario. This sub-sample is used for probing dark matter masses from 10 GeV to 1 TeV. The high-energy sample is produced with a BDT trained for the $m_\chi = 300$ GeV, $\chi \to W^+W^-$ scenario and used to probe dark matter masses from 1 TeV to 40 TeV. The background event distribution is estimated by scrambling data in right ascension, assuming that the background neutrino flux is uniform in right ascension. To account for potential signal contamination in the scrambled data, a signal-subtracted likelihood is used. Details of the analysis method can be found from Reference [26].

The left panel of Figure 4 presents upper limits on the velocity-averaged dark matter annihilation cross-section. The right panel shows lower limits on the dark matter lifetime. They are calculated at 90% C.L. assuming the NFW halo model. The limits from this analysis improve upon the previous best IceCube limits for low dark matter masses.

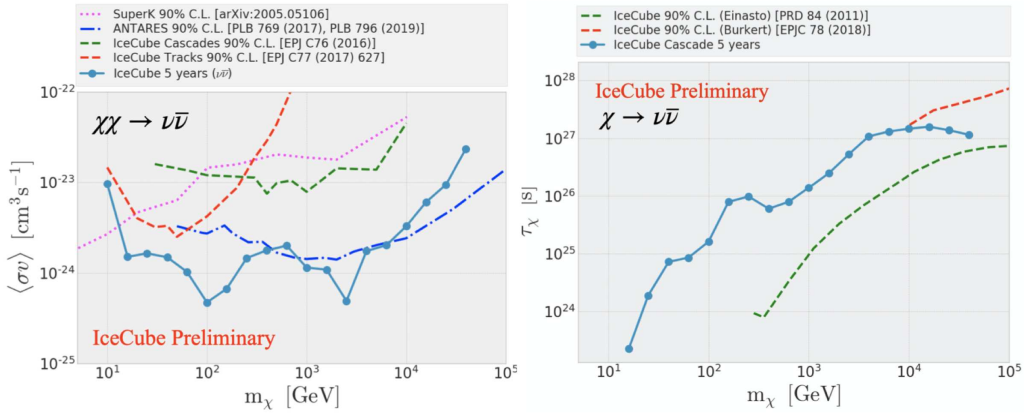

Figure 4. Limits on the velocity-averaged dark matter self-annihilation cross-section (left panel) and the dark matter lifetime (right panel). The solid lines represent the limits obtained from the Neutrino Line analysis at 90% confidence level. They are compared with limits from other neutrino experiments [6,9,10,24,27,28]. The plots are taken from Reference [26].

4. Galactic Center Analysis with OscNext 8-Year Sample

The analysis is being developed to search for low-energy neutrinos from dark matter annihilation in the Galactic Center. The considered dark matter masses range from 5 GeV to 8 TeV. Also, various dark matter annihilation channels are probed.

This work uses 8 years of DeepCore events collected from 2012 to 2020. The data sample is based on the oscNext event selection, which is developed for atmospheric neutrino oscillation measurement. For this particular analysis, the zenith angle cut and energy cut in the original oscNext event selection are released. The signal neutrino spectra corresponding to the considered dark matter masses and channels are obtained from the

PPPC4 [25] table, and the NFW and Burkert halo models discussed in [18] are considered. The background event distribution is estimated using Monte Carlo simulation. Three variables are used as observables: reconstructed energy, angular distance from the Galactic Center, and particle ID (PID) (see Reference [26] for more details of the analysis method).

Figure 5 shows the sensitivities of this analysis to the velocity-averaged dark matter annihilation cross-section. These sensitivities are calculated assuming the NFW model. For the $\nu_e\bar{\nu}_e$, $\nu_\mu\bar{\nu}_\mu$, and $\nu_\tau\bar{\nu}_\tau$ channels, higher dark matter masses than 200 GeV are not considered, as the neutrino spectra consist of a peak at energies to which DeepCore is not sensitive. From the right panel of the figure, it can be seen that the analysis improves upon previous IceCube analyses and ANTARES analyses.

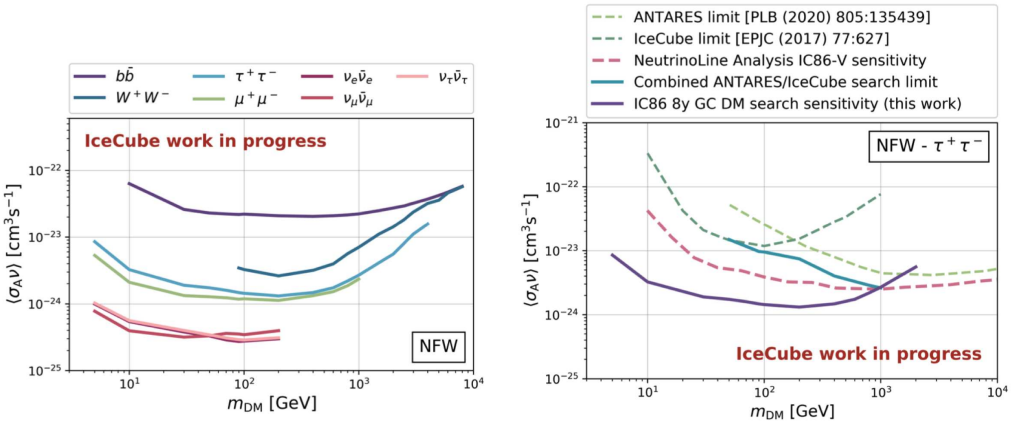

Figure 5. Sensitivities (90% C.L.) of the low-energy Galactic Center analysis to the velocity-averaged dark matter self-annihilation cross-section. Left panel presents the sensitivities calculated for the considered dark matter annihilation channels and the NFW halo model. Right panel shows the sensitivities for the $\tau^+\tau^-$ channel compared with limits from other neutrino experiments [10,11,29]. The plots are taken from [26].

5. Search for Dark Matter Decay in Galaxy Clusters and Galaxies

The analysis is in progress to search for dark matter decay in nearby galaxy clusters and galaxies. This analysis focuses on dark matter with masses from 10 TeV to 100 PeV, decaying through the $b\bar{b}$, W^+W^-, $\tau^+\tau^-$, or the $\nu\bar{\nu}$ channel. Energy and directional information are used as observables. For a given source, dark matter mass, and decay channel, the expected neutrino flux is calculated using Equation (2).

In this work, the neutrino spectra for the considered dark matter masses and decay channels are obtained using the $\chi aro\nu$ package [30]. To calculate the neutrino spectra for higher dark matter masses than 500 GeV, this package adopts the HDMSpectra package [31] that accounts for electroweak corrections. Table 1 lists the targets selected for this analysis, along with their properties. The fifth column from the left shows the angular radius of the region of interest (ROI). The sixth column represents the integral of dark matter density along the line-of-sight and over the solid angle corresponding to θ_{ROI}. For the galaxy clusters and dwarf galaxies, the angular radius, θ_{ROI}, corresponds to the angle where D_{tot} starts to saturate. For the Andromeda galaxy, the ROI is limited to 8° in radius, in order to have a sufficient separation from its ROI to the Galactic Plane. The selected targets are expected to produce a large neutrino flux and are located in the northern sky from which the atmospheric muon backgrounds are effectively absorbed by Earth. The NFW models presented in References [32,33] are used to calculate the spatial distribution of neutrino flux from the galaxy clusters and Andromeda, and the Zhao models in Reference [34] are used for the dwarf galaxies. We disregard the subhalos of dark matter, as the expected neutrino flux from dark matter decay is not highly sensitive to the subhalos. The targets are stacked within the same source class to enhance the analysis sensitivity and mitigate the impact of halo model uncertainties. In order to achieve a good pointing resolution, the analysis uses

a sample of upward-going track-like events, collected from 2012 to 2022. The distribution of background events is estimated from scrambled data in the same way as for the neutrino line analysis discussed in Section 3. To find an excess of events, an unbinned maximum likelihood analysis is conducted.

Sensitivities of the analysis to the dark matter lifetime are presented in Figure 6, along with the limits from previous analyses, including those from other experiments. The solid lines represent the analysis sensitivities obtained by stacking the galaxy clusters, dwarf galaxies, or using the Andromeda galaxy alone. Stacking the galaxy clusters leads to the best sensitivities, which are comparable to the HAWC limits, but extend to higher dark matter masses. The analysis could complement the previous IceCube analyses.

Table 1. Targets selected for the extragalactic decaying dark matter analysis. The third and fourth columns from the left show the right ascension and declination of the targets in equatorial coordinates for epoch J2000. In the fifth column, θ_{ROI} represents the angular radius of the region of interest. D_{tot} is the integral of the dark matter density along the line of sight and over the solid angle corresponding to θ_{ROI}.

Source	Type	RA [°]	Dec [°]	θ_{ROI} [°]	$\log_{10}(D_{tot})$
Virgo	galaxy cluster	186.63	12.72	6.11	20.40
Coma	galaxy cluster	194.95	27.94	1.30	19.17
Perseus	galaxy cluster	49.94	41.51	1.35	19.15
Andromeda	galaxy	10.68	41.27	8.00	20.23
Draco	dwarf galaxy	260.05	57.92	1.30	18.97
Ursa Major II	dwarf galaxy	132.87	63.13	0.53	18.39
Ursa Minor	dwarf galaxy	227.28	67.23	1.32	18.13
Segue 1	dwarf galaxy	151.77	16.08	0.34	17.99
Coma Berenices	dwarf galaxy	186.74	23.9	0.34	17.96
Leo I	dwarf galaxy	152.12	12.3	0.45	17.92
Boötes I	dwarf galaxy	210.03	14.5	0.53	17.90

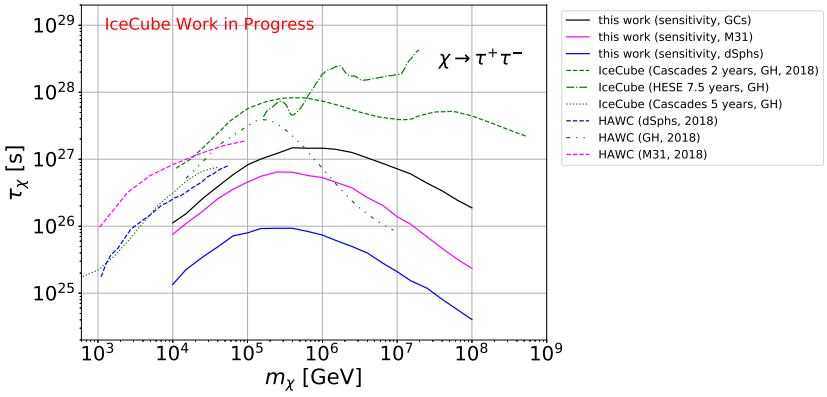

Figure 6. Sensitivities of the extragalactic decaying dark matter analysis to the dark matter lifetime. The solid lines represent the sensitivities of the analysis, calculated at 90% confidence level. The other lines are limits from recent IceCube and HAWC analyses [16,23,24,35–37]. The confidence levels associated with the IceCube and HAWC limits are 90% and 95%, respectively.

6. Conclusions

We presented dark matter searches with IceCube, which were recently completed or are in progress. The analyses using the HESE 7.5-year sample derived strong constraints on dark matter annihilation, decay, and dark matter–neutrino scattering. The neutrino line analysis improved upon the previous best IceCube limits on both dark matter annihilation and decay for low dark matter masses. The Galactic Center analysis with the oscNext 8-year sample is expected to be an improvement over previous IceCube results for low

dark matter masses. Lastly, the search for dark matter decay in nearby galaxy clusters and galaxies is expected to complement previous decaying dark matter searches with IceCube. The results of these ongoing analyses will be discussed in future publications.

Funding: This research received no external funding.

Institutional Review Board Statement: Not applicable.

Informed Consent Statement: Not applicable.

Data Availability Statement: The data are not publicly available due to collaboration policies. The IceCube Collaboration decides when data is released.

Acknowledgments: The support and resources from the Center for High Performance Computing at the University of Utah are gratefully acknowledged.

Conflicts of Interest: The author declares no conflict of interest.

References

1. Aartsen, M.G.; Ackermann, M.; Adams, J.; Aguilar, J.A.; Ahlers, M.; Ahrens, M.; Altmann, D.; Andeen, K.; Anderson, T.; Ansseau, I.; et al. The IceCube Neutrino Observatory: Instrumentation and Online Systems. *J. Instrum.* **2017**, *12*, P03012. [CrossRef]
2. Aartsen, M.G.; Ackermann, M.; Adams, J.; Aguilar, J.A.; Ahlers, M.; Ahrens, M.; Altmann, D.; Andeen, K.; Anderson, T.; Ansseau, I.; et al. Search for annihilating dark matter in the Sun with 3 years of IceCube data. *Eur. Phys. J. C* **2017**, *77*, 146; Erratum in *Eur. Phys. J. C* **2019**, *79*, 214. [CrossRef]
3. Abbasi, R.; Ackermann, M.; Adams, J.; Aguilar, J.A.; Ahlers, M.; Ahrens, M.; Alameddine, J.M.; Alispach, C.; Alves, A.A., Jr.; Amin, N.M.; et al. Search for GeV-scale dark matter annihilation in the Sun with IceCube DeepCore. *Phys. Rev. D* **2022**, *105*, 062004. [CrossRef]
4. Aartsen, M.G.; Abraham, K.; Ackermann, M.; Adams, J.; Aguilar, J.A.; Ahlers, M.; Ahrens, M.; Altmann, D.; Andeen, K.; Anderson, T.; et al. First search for dark matter annihilations in the Earth with the IceCube Detector. *Eur. Phys. J. C* **2017**, *77*, 82. [CrossRef]
5. Abbasi, R.; Ackermann, M.; Adams, J.; Aguilar, J.; Ahlers, M.; Ahrens, M.; Alispach, C.M.; Junior, A.A.A.; Amin, N.M.B.; An, R.; et al. Search for dark matter from the center of the Earth with 8 years of IceCube data. In Proceedings of the 37th International Cosmic Ray Conference (ICRC 2021), Berlin, Germany, 12–23 July 2021; p. 526. [CrossRef]
6. Abbasi, R.; Abdou, Y.; Abu-Zayyad, T.; Adams, J.; Aguilar, J.A.; Ahlers, M.; Andeen, K.; Auffenberg, J.; Bai, X.; Baker, M.; et al. Search for dark matter from the Galactic halo with the IceCube Neutrino Telescope. *Phys. Rev. D* **2011**, *84*, 022004. [CrossRef]
7. Abbasi, R.; Abdou, Y.; Ackermann, M.; Adams, J.; Aguilar, J.A.; Ahlers, M.; Altmann, D.; Andeen, K.; Auffenberg, J.; Bai, X.; et al. Search for Neutrinos from Annihilating Dark Matter in the Direction of the Galactic Center with the 40-String IceCube Neutrino Observatory. *arXiv* **2012**, arXiv:1210.3557.
8. Aartsen, M.G.; Abraham, K.; Ackermann, M.; Adams, J.; Aguilar, J.A.; Ahlers, M.; Ahrens, M.; Altmann, D.; Anderson, T.; Archinger, M.; et al. Search for Dark Matter Annihilation in the Galactic Center with IceCube-79. *Eur. Phys. J. C* **2015**, *75*, 492. [CrossRef]
9. Aartsen, M.G.; Abraham, K.; Ackermann, M.; Adams, J.; Aguilar, J.A.; Ahlers, M.; Ahrens, M.; Altmann, D.; Andeen, K.; Anderson, T.; et al. All-flavour Search for Neutrinos from Dark Matter Annihilations in the Milky Way with IceCube/DeepCore *Eur. Phys. J. C* **2016**, *76*, 531. [CrossRef]
10. Aartsen, M.G.; Ackermann, M.; Adams, J.; Aguilar, J.A.; Ahlers, M.; Ahrens, M.; Al Samarai, I.; Altmann, D.; Andeen, K.; Anderson, T.; et al. Search for Neutrinos from Dark Matter Self-Annihilations in the center of the Milky Way with 3 years of IceCube/DeepCore *Eur. Phys. J. C* **2017**, *77*, 627. [CrossRef]
11. Albert, A.; André, M.; Anghinolfi, M.; Ardid, M.; Aubert, J.-J.; Aublin, J.; Baret, B.; Basa, S.; Belhorma, B.; Bertin, V.; et al. Combined search for neutrinos from dark matter self-annihilation in the Galactic Center with ANTARES and IceCube. *Phys. Rev. D* **2020**, *102*, 082002. [CrossRef]
12. Aartsen, M.G.; Abbasi, R.; Abdou, Y.; Ackermann, M.; Adams, J.; Aguilar, J.A.; Ahlers, M.; Altmann, D.; Auffenberg, J.; Bai, X.; et al. IceCube Search for Dark Matter Annihilation in nearby Galaxies and Galaxy Clusters. *Phys. Rev. D* **2013**, *88*, 122001. [CrossRef]
13. Abbasi, R.; Abdou, Y.; Abu-Zayyad, T.; Adams, J.; Aguilar, J.A.; Ahlers, M.; Andeen, K.; Auffenberg, J.; Bai, X.; Baker, M.; et al. The IceCube high-energy starting event sample: Description and flux characterization with 7.5 years of data. *Phys. Rev. D* **2021**, *104*, 022002. [CrossRef]
14. Vincent, A.C.; Martin, P.; Cline, J.M. Interacting dark matter contribution to the Galactic 511 keV gamma ray emission: Constraining the morphology with INTEGRAL/SPI observations. *J. Cosmol. Astropart. Phys.* **2012**, *4*, 022. [CrossRef]
15. Einasto, J. On the Construction of a Composite Model for the Galaxy and on the Determination of the System of Galactic Parameters. *Trudy Astrofiz. Instituta Alma-Ata* **1965**, *5*, 87–100.

16. Abbasi, R.; Ackermann, M.; Adams, J.; Aguilar, J.A.; Ahlers, M.; Ahrens, M.; Alameddine, J.M.; Alves, A.A., Jr.; Amin, N.M.; Andeen, K.; et al. Searches for Connections between Dark Matter and High-Energy Neutrinos with IceCube. *arXiv* **2022**, arXiv:2205.12950.
17. Sjostrand, T.; Mrenna, S.; Skands, P.Z. A Brief Introduction to PYTHIA 8.1. *Comput. Phys. Commun.* **2008**, *178*, 852–867. [CrossRef]
18. Nesti, F.; Salucci, P. The Dark Matter halo of the Milky Way, AD 2013. *J. Cosmol. Astropart. Phys.* **2013**, *7*, 016. [CrossRef]
19. Albert, A.; AndrÃ©, M.; Anghinolfi, M.; Anton, G.; Ardid, M.; Aubert, J.J.; Avgitas, T.; Baret, B.; Barrios-MartÃ, J.; Basa, S.; et al. Results from the search for dark matter in the Milky Way with 9 years of data of the ANTARES neutrino telescope. *Phys. Lett. B* **2017**, *769*, 249–254. [CrossRef]
20. Aliu, E.; Archambault, S.; Arlen, T.; Aune, T.; Beilicke, M.; Benbow, W.; Bouvier, A.; Bradbury, S.M.; Buckley, J.H.; Bugaev, V.; et al. VERITAS Deep Observations of the Dwarf Spheroidal Galaxy Segue 1. *Phys. Rev. D* **2012**, *85*, 062001; Erratum in *Phys. Rev. D* **2015**, *91*, 129903. [CrossRef]
21. MAGIC Collaboration. Limits to Dark Matter Annihilation Cross-Section from a Combined Analysis of MAGIC and Fermi-LAT Observations of Dwarf Satellite Galaxies. *J. Cosmol. Astropart. Phys.* **2016**, *2*, 039.
22. Abdallah, H.; Abramowski, A.; Aharonian, F.; Benkhali, F.A.; Akhperjanian, A.G.; Angüner, E.; Arrieta, M.; Aubert, P.; Backes, M.; Balzer, A.; et al. Search for dark matter annihilations towards the inner Galactic halo from 10 years of observations with H.E.S.S. *Phys. Rev. Lett.* **2016**, *117*, 111301. [CrossRef] [PubMed]
23. Albert1, A.; Alfaro, R.; Alvarez, C.; Álvarez, J.D.; Arceo, R.; Arteaga-Velázquez, J.C.; Rojas, D.A.; Solares, H.A.A.; Bautista-Elivar, N.; Becerril, A.; et al. Dark Matter Limits From Dwarf Spheroidal Galaxies with The HAWC Gamma-Ray Observatory. *Astrophys. J.* **2018**, *853*, 154. [CrossRef]
24. Aartsen, M.G.; Ackermann, M.; Adams, J.; Aguilar, J.A.; Ahlers, M.; Ahrens, M.; Samarai, I.A.; Altmann, D.; Andeen, K.; Anderson, T.; et al. Search for neutrinos from decaying dark matter with IceCube. *Eur. Phys. J. C* **2018**, *78*, 831. [CrossRef] [PubMed]
25. Cirelli, M.; Corcella, G.; Hektor, A.; HÃ¼tsi, G.; Kadastik, M.; Panci, P.; Raidal, M.; Sala, F.; Strumia, A. PPPC 4 DM ID: A poor particle physicist cookbook for dark matter indirect detection. *J. Cosmol. Astropart. Phys.* **2011**, *2011*, 051. [CrossRef]
26. Iovine, N. Dark matter searches in the centre of the Milky Way with IceCube. In Proceedings of the 41st International Conference on High Energy Physics (ICHEP2022), Bologna, Italy, 6–13 July 2022; p. 311. [CrossRef]
27. Abe, K.; Bronner, C.; Haga, Y.; Hayato, Y.; Ikeda, M.; Imaizumi, S.; Ito, H.; Iyogi, K.; Kameda, J.; Kataoka, Y.; et al. Indirect search for dark matter from the Galactic Center and halo with the Super-Kamiokande detector. *Phys. Rev. D* **2020**, *102*, 072002. [CrossRef]
28. Albert, A.; André, M.; Anghinolfi, M.; Anton, G.; Ardid, M.; Aubert, J.-J.; Avgitas, T.; Baret, B.; Barrios-Martí, J.; Basa, S.; et al. Results from the search for dark matter in the Milky Way with 9 years of data of the ANTARES neutrino telescope. *Phys. Lett. B* **2017**, *769*, 249; Erratum in *Phys. Lett. B* **2019**, *796*, 253. [CrossRef]
29. Albert, A.; André, M.; Anghinolfi, M.; Anton, G.; Ardid, M.; Aubert, J.-J.; Aublin, J.; Baret, B.; Basa, S.; Belhorma, B.; et al. Search for dark matter towards the Galactic Centre with 11 years of ANTARES data. *Phys. Lett. B* **2020**, *805*, 135439. [CrossRef]
30. Liu, Q.; Lazar, J.; Argüelles, C.A.; Kheirandish, A. χaroν: A tool for neutrino flux generation from WIMPs. *J. Cosmol. Astropart. Phys.* **2020**, *10*, 043. [CrossRef]
31. Bauer, C.W.; Rodd, N.L.; Webber, B.R. Dark matter spectra from the electroweak to the Planck scale. *J. High Energy Phys.* **2021**, *6*, 121. [CrossRef]
32. Sanchez-Conde, M.A.; Cannoni, M.; Zandanel, F.; Gomez, M.E.; Prada, F. Dark matter searches with Cherenkov telescopes: nearby dwarf galaxies or local galaxy clusters? *J. Cosmol. Astropart. Phys.* **2011**, *12*, 011. [CrossRef]
33. Tamm, A.; Tempel, E.; Tenjes, P.; Tihhonova, O.; Tuvikene, T. Stellar mass map and dark matter distribution in M31. *Astron. Astrophys.* **2012**, *546*, A4. [CrossRef]
34. Geringer-Sameth, A.; Koushiappas, S.M.; Walker, M. Dwarf galaxy annihilation and decay emission profiles for dark matter experiments. *Astrophys. J.* **2015**, *801*, 74. [CrossRef]
35. Aguilar, J.A. Searches of New Physics with the IceCube Neutrino Observatory. In Proceedings of the International Conference on Neutrinos and Dark Matter (NuDM-2022), Sharm El Sheikh, Egypt, 25–28 September 2022.
36. Abeysekara, A.U.; Albert, A.; Alfaro, R.; Alvarez, C.; Arceo, R.; Arteaga-Velázquez, J.C.; Rojas, D.A.; Solares, H.A.A.; Becerril, A.; Belmont-Moreno, E.; et al. A Search for Dark Matter in the Galactic Halo with HAWC. *J. Cosmol. Astropart. Phys.* **2018**, *2*, 049. [CrossRef]
37. Albert, A.; Alfaro, R.; Alvarez, C.; Álvarez, J.D.; Arceo, R.; Arteaga-Velázquez, J.C.; Rojas, D.A.; Solares, H.A.A.; Becerril, A.; Belmont-Moreno, E.; et al. Search for Dark Matter Gamma-ray Emission from the Andromeda Galaxy with the High-Altitude Water Cherenkov Observatory. *J. Cosmol. Astropart. Phys.* **2018**, *6*, 043; Erratum in *J. Cosmol. Astropart. Phys.* **2019**, *4*, E01. [CrossRef]